

Cover Page



Universiteit Leiden



The handle <http://hdl.handle.net/1887/42846> holds various files of this Leiden University dissertation.

Author: Wiekmeijer A.S.

Title: In vivo modelling of normal and pathological human T-cell development

Issue Date: 2016-09-08

Chapter 4

Identification of a novel type of T-B⁺SCID with a late double positive thymic arrest

Anna-Sophia Wiekmeijer¹, Gertjan Driessen², Karin Pike-Overzet¹, Martijn H. Brugman¹, Gijs W.E. Santen³, Sandra A. Vloemans¹, Wibowo Arindrarto⁴, Erdogan Taskesen^{5,6}, Marcel J.T. Reinders^{5,6}, Rogier Kersseboom⁷, Jasper J. Saris⁷, Renske Oegema⁷, Robbert G.M. Bredius⁸, Mirjam van der Burg³, Frank J.T. Staal¹

¹Department of Immunohematology and Blood Transfusion, Leiden University Medical Center, Leiden, The Netherlands

²Department of Immunology, Erasmus MC, University Medical Center Rotterdam, Rotterdam, The Netherlands

³Department of Clinical Genetics, Leiden University Medical Center, Leiden, The Netherlands

⁴Sequence Analysis Support Core, Leiden University Medical Center, Leiden, The Netherlands

⁵Delft Bioinformatics Lab (DBL), Delft University of Technology, Delft, The Netherlands

⁶Netherlands Bioinformatics Centre (NBIC), The Netherlands

⁷Department of Clinical Genetics, Erasmus MC, University Medical Center Rotterdam, Rotterdam, The Netherlands

⁸Department of Pediatrics, Leiden University Medical Center, Leiden, The Netherlands

Manuscript in preparation

Abstract

More than 16 genes have been shown to be causative for severe combined immunodeficiency (SCID). However, around 20% of patients remain without molecular diagnosis. Here, we present data on a female patient with an atypical presentation of SCID whose initial diagnosis was hard to make. By transplantation of patient derived hematopoietic stem and progenitor cells in immunodeficient mice, we could demonstrate that this case was a T^B⁺NK⁺-SCID. Phenotypic analysis of the thymocytes of these mice demonstrated an arrest in T-cell development at the CD3⁻ to CD3⁺-CD4⁺CD8⁺ double positive and the subsequent CD4⁻ and CD8⁻-single positive transition. Using whole exome sequencing, we identified a *de novo* heterozygous missense mutation in *VPS4B* that potentially could lead to SCID with atypical presentation.

Introduction

Severe combined immunodeficiency (SCID) is a congenital disorder that is characterized by a deficiency of T cells in peripheral blood (PB). This deficiency in T cells can be accompanied by defects in either B or NK cells or both and can be categorized in 2 groups: T^B⁻-SCID and T^B⁻-SCID^{1,2}. SCID affects approximately 1 in 100,000 live births and the patients present, mostly within their first year of life, with opportunistic infections and a failure to thrive^{3,4}. Currently, the best treatment option is a hematopoietic stem cell transplantation (HSCT) although clinical trials are ongoing with gene therapy approaches for SCID caused by mutations in either *IL2RG* or *ADA*^{5,6,7,8,9}. Patients suffering from SCID caused by a mutation in *ADA* also benefit from enzyme replacement therapy¹⁰. Besides *IL2RG* and *ADA*, many genes can underlie this disease; up to now more than 16 have been described^{2,10}. However, a substantial fraction of patients without an identified disease-causing mutation is still remaining. Different fractions of SCID patients without a molecular diagnosis have been reported, ranging from 7 to 33%^{10,11,12,13,14}.

A new approach to search for disease-causing genes is whole exome sequencing. This can be done by sequencing the coding sequences of the genome of a group of patients, as has been shown for Bartter Syndrome¹⁵ and Miller Syndrome¹⁶. Due to the rarity of SCID, especially the ones without a molecular diagnosis, it is very difficult to obtain a patient group for exome sequencing with the same molecular defect. In these cases whole exome sequencing of a single patient and both parents can be useful, in which the exome of the patient and both parents are compared to exclude inherited non-damaging single nucleotide variations (SNVs), instead of multiple patients and a control group. This approach has proven successful, for instance, by demonstrating that a mutation in *CARD11* causes SCID¹⁷.

Here, we report on a patient with atypical presentation of SCID. Using the novel approach of transplanting patient derived hematopoietic stem and progenitor cells (HSPCs) in the NOD/Scid-*Il2rg*^{-/-} (NSG) mouse model, we could demonstrate that this patient has a hematopoietic cell-intrinsic defect and identified the stage of arrest in T-cell development. Using exome sequencing combined with whole exome sequencing analysis of patient and both parents we identified a *de novo* mutation in *VPS4B* that might be causative for T^B⁺NK⁺-SCID as it is predicted to act as dominant negative molecule.

Materials and methods

Human CD34⁺ bone marrow derived cells

Human bone marrow (BM) was obtained from healthy pediatric BM donors at the Leiden University Medical Center (LUMC, Leiden, The Netherlands). Informed consent was obtained from the parents for the use of leftover samples for research purposes. BM from the patient was obtained according to the guidelines of the Erasmus MC. The medical ethical committees of LUMC and of Erasmus MC approved this study and both served as institutional review boards. Informed consent was provided according to the Declaration of Helsinki. Mononuclear cells were isolated using Ficoll gradient centrifugation, frozen in fetal calf serum (FCS)/10% DMSO (Greiner Bio-One B.V., Alphen aan den Rijn, The Netherlands and Sigma-Aldrich, St. Louis, MO, USA, respectively) and stored in liquid nitrogen. Cells were isolated and cultured as described previously¹⁸.

Mice

NOD.Cg-Prkdc^{scid} Il2rg^{tm1Wjl}/SzJ (NSG) mice were obtained from Charles River Laboratories (Kent, United Kingdom) and bred in the animal facility at the Leiden University Medical Center. Experimental procedures were approved by the Ethical Committee on Animal Experiments of the LUMC. Female NSG mice were transplanted with CD34⁺ cells by intravenous injection within 24 hours after irradiation with 1.91 Gy using orthovoltage X-rays as described previously^{18,19}. Mice transplanted with CD34⁺ cells derived from healthy pediatric bone marrow are historical controls, due to the rarity of this material, and have been described elsewhere¹⁹.

Flow cytometry

Analysis of lymphocyte populations in peripheral blood and composition of the B-cell precursor compartment in the BM of the patient was performed as previously described²⁰.

Labeling of mononuclear cells of transplanted NSG mice has been described¹⁸. The following anti-human antibodies were used: CD3-PECy5 (UCHT1), CD4-APCCy7 (RPA-T4), CD5-FITC (UCHT2), CD7-PECy5 (M-T701), CD8-PECy7 (SK1), CD13-APC (WM15), CD16-PE (B73.1), CD19-APCCy7 (SJ25C1), CD20-PE (L27), CD33-APC (WM53), CD34-PE (8G12), CD45-V450, CD56-PE (MY31), TCRαβ-PE (T10B9.1A-31), streptavidin-PerCPCy5.5 (all from BD Biosciences, San Jose, CA) and CD10-biotin (eBioCB-CALLA) (eBioscience, San Diego, CA). Data were acquired on a Canto II (BD Biosciences) and analyzed using FlowJo software (Treestar, Ashland, OR, USA).

Sequence analysis

DNA was isolated from peripheral blood mononuclear cells from patient and both parents using the GeneElute™ Mammalian Genomic DNA Miniprep Kit (Sigma Aldrich, St. Louis, MO, USA) according to the manufacturer's protocol. Sanger sequencing of known genes causative for SCID (*ADA*, *RAG1*, *RAG2*, *IL2RG*, *CD3D*, *CD3E*, *CD3G*, and *CD3Z/CD247*) was performed by PCR analysis (primers and amplification protocol are available upon request). The following primers were used for amplification and Sanger sequencing of the *VPS4B* gene: Forward 5'-ATCTGGGAGATTTGATTCAT-3', Reverse 5'-ATGAAAGACAGAAGTGTGTG-3'. Amplification was performed using the following protocol: 2 minutes 94°C, followed by 35 cycles of 94°C 15 seconds, 60°C 30 seconds, 72°C 2 minutes, followed by 10 minutes at 72°C. Products were

separated on a 2% gel and fragments were isolated using the Zymoclean Gel DNA Recovery Kit (Zymo Research Corporation, Irvine, CA, USA) for Sanger sequencing.

Whole exome sequencing

Exome sequencing was performed at GATC BioTech (Constance, Germany) using Agilent SureSelect post-capture and enrichment protocols together with Illumina HiSeq 2500 platform. Reads were aligned using an in-house developed GNU Makefile-based pipeline ('Magpie', <https://git.lumc.nl/rig-framework/magpie>), based on the GATK 2.7 best practices²¹. Briefly, each FASTQ pair was processed using Sickle (version 1.33, <https://github.com/najoshi/sickle>) with default settings to trim low-quality bases. Remaining reads were mapped to the hg19 human genome sequence using Burrows-Wheeler Aligner (BWA)-MEM (version 0.7.5)²². The resulting alignment was then compressed using the Samtools (version 0.1.19) suite²³. Duplicates were removed using Picard Mark Duplicates (<https://broadinstitute.github.io/picard/>) and data was subsequently processed through the GATK tools RealignTargetCreator, IndelRealigner, BaseRecalibrator, and PrintReads according to the GATK version 2.7 best practices and using the provided GATK 2.5 data bundle. The resulting alignment file was then used as input for the GATK variant callers HaplotypeCaller and UnifiedGenotyper, followed by variant recalibration. The generated VCF file was annotated using the SeattleSeq web service (<http://snp.gs.washington.edu/SeattleSeqAnnotation141/>) and various other publically available databases (see results).

Results

Clinical presentation of the patient

The patient was a girl born at gestational age of 39 weeks and 5 days with a birth weight of 4120 g. Her parents were non-consanguineous and the pregnancy was without complications. At the age of 5 months she was admitted to the hospital for failure to thrive. An auto-immune thyroiditis with hypothyroidism was detected and levothyroxine treatment was initiated. Nine months later, at the age of one year and two months, she developed a severe bronchiolitis secondary to a bocavirus and adenovirus infection. Because of respiratory failure she was admitted to the intensive care unit and subsequently developed progressive respiratory failure during mechanical ventilation, for which she was treated with extra-corporal membrane oxygenation (ECMO) for 5 days. During ECMO two infusions of high dose methylprednisolone were given. Bronchoscopy showed trachomalacia of the right main bronchus. Immunological examination revealed a severe T-cell cytopenia (Fig. 1A), B-cell cytopenia (Fig. 1B) and a mild hypogammaglobulinemia (IgG: 2.5 g/L, IgA: 0.56 g/L, IgM: < 0.3 g/L). NK cell numbers were low at diagnosis but recovered quickly (Fig. 1C). Initially these abnormalities were thought to result from methylprednisolone treatment, but T-cell lymphopenia persisted, whereas B-cell and NK-cell lymphopenia recovered (Fig. 1A-C). At the time when B-cell numbers were spontaneously recovered, examination of the bone marrow showed no block in precursor B-cell development (Fig. 1D). Response to booster vaccination with tetanus, diphtheria and polio was normal, but no response could be detected to pneumococcal conjugate vaccine.

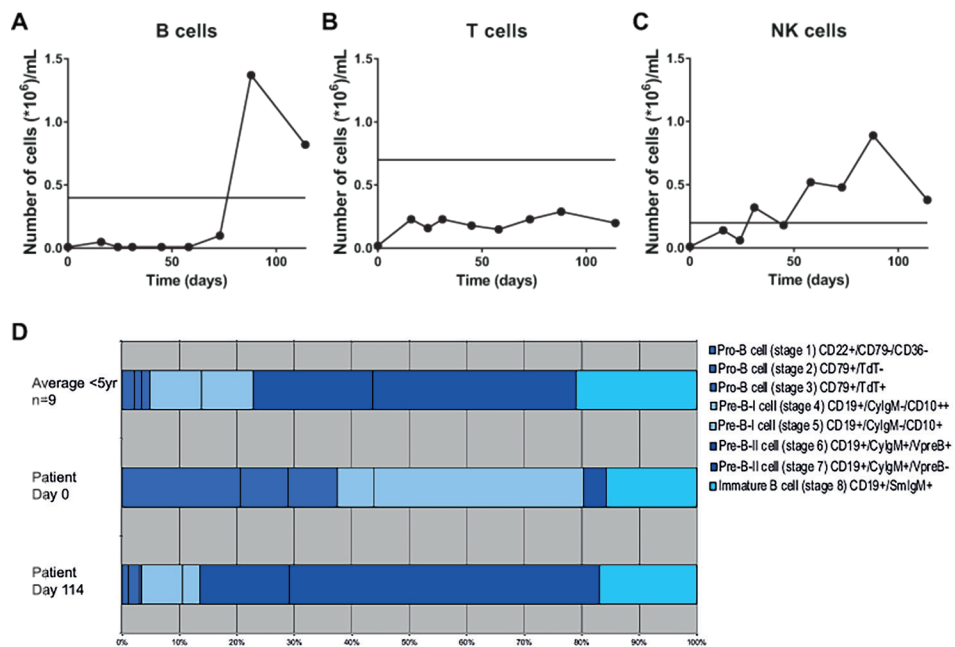


Figure 1: Lymphocyte characteristics in suspected SCID patient. **A)** B cell counts in peripheral blood of patient over time. **B)** T cell counts in peripheral blood of patient over time. **C)** NK cell counts in peripheral blood of patient over time. **A-C)** Horizontal lines indicate reference values. **D)** Developmental stages of B cell progenitors in BM of patient at two time points and of healthy controls.

Suspicion of SCID

Due to the persisting T-cell lymphopenia there was a suspicion of SCID and therefore genetic and metabolic analysis for ADA and PNP deficiency was initiated, but this showed no abnormalities. Also in the *RAG1* and *RAG2* genes no pathogenic mutations could be detected (data not shown). On karyotyping examination the patient was chromosomally 46,XY. External genital organs had a normal female appearance, except for partial fusion of the labia minora, and abdominal ultrasound revealed the presence of a uterus, but ovaries or testes could not be detected. Diagnostic SNP-array CGH analysis confirmed the chromosomal 46,XY and reported a heterozygous 450kb 4q23 micro-deletion (arr[hg18] ch4:108.60-109.05) of unknown clinical relevance. This variant was also present in her father and therefore presumed unlikely to be pathogenic. Subsequent *IL2RG* analysis was normal (data not shown).

Because of suspected SCID she was treated with (intravenous and later subcutaneous) intravenous immunoglobulin (IVIG) substitution, cotrimoxazol and valaciclovir prophylaxis. For the hypogonadism, treatment with sex hormones was given. Post ECMO she developed recurrent convulsions with multifocal epileptic activity and a delirium, for which she was treated with anti-epileptic drugs (levetiracetam) and haloperidol.

At the age of one year and seven months she underwent a HSCT from her HLA-identical brother. Post transplantation she developed a severe Coombs positive hemolytic anemia for which high dose IVIG, methylprednisolon, rituximab and erythrocyte transfusions were given. Because no donor chimerism was present a second HSCT with the same donor was performed, which resulted in 100% donor chimerism. Post HSCT, ongoing hemolysis was treated with bortezomib and adenovirus reactivation with cidofovir. Later, she developed a progressive severe neurological deterioration; no spontaneous motor activity or tendon reflexes could be detected, and responses to visually evoked potentials were absent. CSF examination revealed no abnormalities. Cerebral MRI showed generalized atrophy and leukoencephalopathy. Next, she developed a severe lower respiratory infection that was fatal. Post mortal examination of the brain showed severe encephalopathy and gliosis, without signs of inflammation or infection.

T-cell deficiency is caused by a cell intrinsic defect

Patient derived hematopoietic stem and progenitor cells (HSPCs) were isolated from a cryopreserved BM aspirate taken at the time when B-cell numbers had recovered. The HSPCs were transplanted in NSG mice to determine whether the immunological defects that were observed in the patient were caused by niche/stromal defects or by a hematopoietic cell intrinsic deficiency. Previously, we have used this approach to determine the arrests in T-cell development for different types of SCID that were caused by different known underlying genetic defects¹⁹. During follow-up of the mice transplanted with patient-derived HSPCs, there was outgrowth of both myeloid and B cells in peripheral blood, but T cells were not detected at any of the time points, whereas in mice transplanted with normal control HSPCs T cells were readily detected (Fig. 2A). In addition, at the end of the experiment, T cells were hardly detectable in mice transplanted with patient-derived HSPCs while they were present in UCB and BM transplanted control NSG mice (Fig. 2B, C). Taken together, the phenotype observed in mice transplanted with patient-derived HSPCs was consistent with a T-B⁺-SCID diagnosis.

Arrest in T-cell development at DP stage

As virtually no T cells could be detected in peripheral blood of both the patient and NSG mice transplanted with patient derived HSPCs, we examined T-cell developmental stages in thymi of transplanted NSG mice. Total thymocyte counts did not differ between mice transplanted with patient derived HSPCs or control HSPCs (Fig. 3A). We then analyzed the thymus of transplanted NSG mice for the presence of the different stages of T-cell development. The percentage of both mature CD4⁺ single positive (SP) and CD8⁺ SP was drastically decreased when patient derived HSPCs were transplanted (Fig. 3B, C). Furthermore the percentage of CD3⁺ CD4⁺ CD8⁺ double positive (DP) cells was lower while there was an increase in the percentage of CD3⁺ DP cells. The level of both CD3 and TCR $\alpha\beta$ expression was decreased in the total thymocyte population as compared to mice transplanted with UCB derived HSPCs (Fig. 3D). In addition, no CD5^{hi} expressing cells could be detected (Fig. 3E), a molecule known to be upregulated upon TCR signaling²⁴. From these phenotypic data, we could confirm that this patient suffered from SCID. Together these data point to an arrest in development that is most pronounced at the CD3⁺ DP to SP transition while there might also be problems in TCR expression and signaling, as indicated by the increase in CD3⁺ DP and decrease of CD3⁺ DP (Fig. 3C).

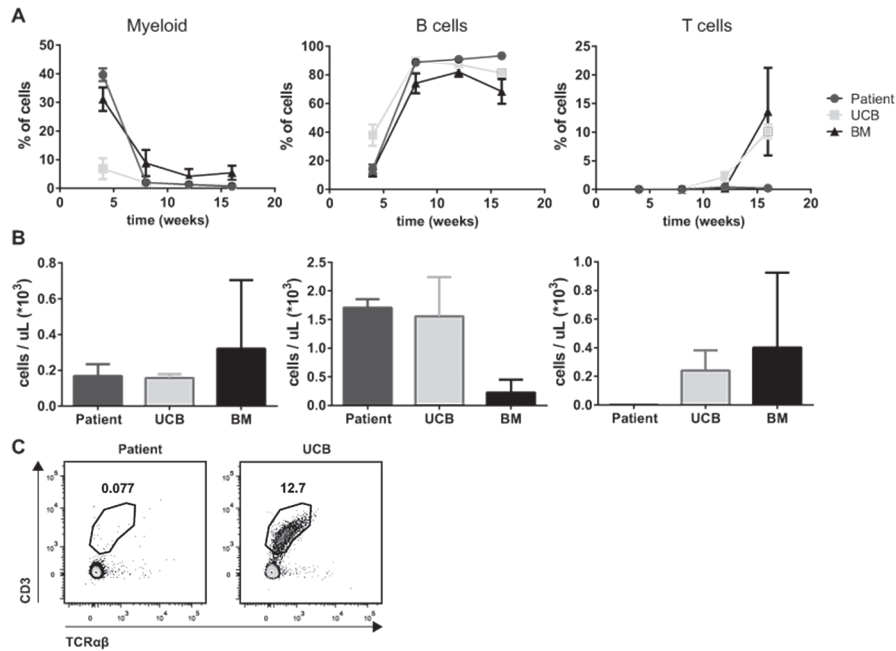


Figure 2: T-cell deficiency is caused by a hematopoietic cell intrinsic defect. **A)** Percentages of cells from different lineages in peripheral blood of NSG mice transplanted with HSPCs from patient or control UCB and BM. Percentages are within hCD45⁺ mononuclear cell fraction. **B)** Cell counts of cells from different lineages in peripheral blood of NSG mice at the end of the experiment. **C)** FACS plots showing CD3 and TCRαβ expression in peripheral blood of NSG mice at the end of the experiment. Cells were gated within hCD45⁺ mononuclear cell fraction.

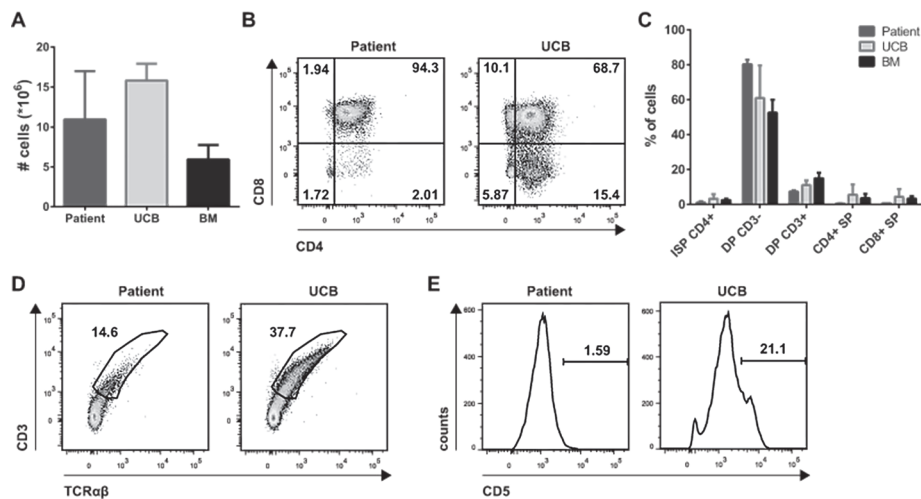


Figure 3: T-cell development is arrested at the transition from CD3⁺ DP to SP. **A)** Absolute cell numbers of total thymocytes. **B)** FACS plots depicting CD8 and CD4 expression on mononuclear hCD45⁺ thymocytes in thymi of transplanted NSG mice. **C)** Frequencies of cells from different T-cell developmental stages within hCD45⁺ cells in thymi of transplanted NSG mice. **D)** Expression of CD3 and TCRαβ within hCD45⁺ cells in thymi of transplanted NSG mice. **E)** Expression of CD5 within hCD45⁺ cells in thymi of transplanted NSG mice.

NK cells were present both in PB and BM (Fig. 4A, B) and no aberrancies were detected within the B-cell compartment in the BM of transplanted NSG mice (Fig. 4C), further supporting that this patient is a T^hB⁺NK⁺SCID.

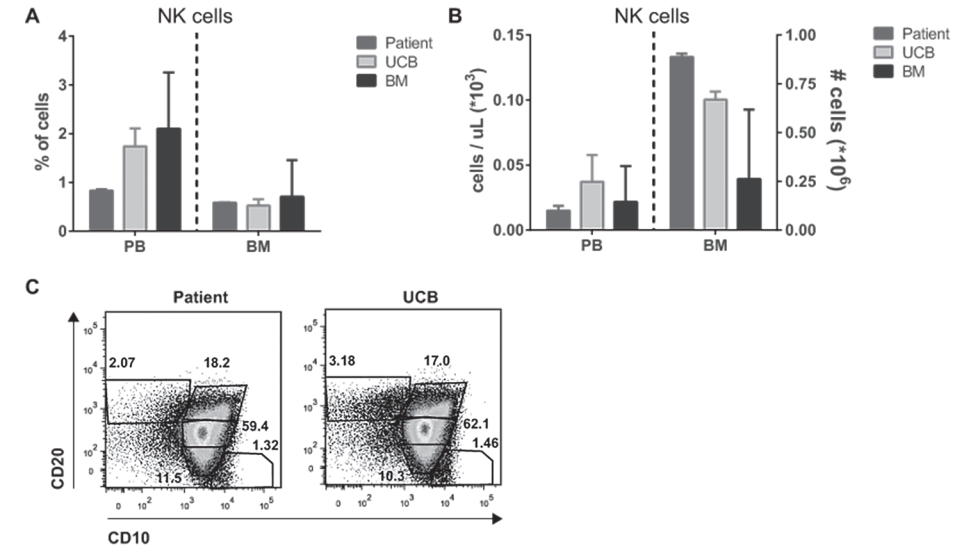


Figure 4: No aberrancies in NK cells and B cells in NSG mice transplanted with patient derived HSPCs. **A)** Percentages and **B)** numbers of NK cells (CD16/56⁺CD13/33⁺) in peripheral blood and bone marrow of NSG mice. Percentages are within hCD45⁺ mononuclear cell fraction. **C)** B-cell developmental stages characterized by expression of CD20 and CD10 in bone marrow of NSG mice. Fractions are within hCD45⁺CD19⁺ mononuclear cell fraction.

Causative genetic defect

Since the arrest in T-cell development was most profound at the DP stage, percentages of CD3 expressing cells were lower and CD5^{hi} expressing thymocytes were absent, mutations in one of the genes encoding the CD3 complex were suspected. Previous analysis had demonstrated that no abnormalities were present in *ADA*, *PNP*, *RAG1*, *RAG2* or *IL2RG*. Therefore, we used Sanger sequencing to determine whether mutations were present in any of the genes encoding the different CD3 chains. No mutations were detected in *CD3D*, *CD3E*, *CD3G* or *CD247* (*CD3Z*) (data not shown). As other SCID genes had been excluded during diagnosis, exome sequencing was performed on DNA of the patient and both parents. Trio-analysis was performed using the Modular GATK Pipeline (Magpie), which is a variant-calling pipeline based on GATK best practice recommendations to analyze multiple samples simultaneously. More than 177 million raw reads were obtained. Almost 164 million reads (92.5%) were uniquely aligned to hg19 using Burrows-Wheeler Aligner (BWA). Median exome coverage was 61-fold both for the exome of the mother and the patient and 57-fold for the reads obtained from the father. In the patient, 381712 SNVs were identified (Fig. 5A). SNVs were called using both HaplotypeCaller and UnifiedGenotyper from the Genome Analysis Toolkit (GATK). High-quality non-synonymous variants in exons were filtered out and sequentially we only filtered for SNVs that were not

present in either dbSNP (v137) or in the 1000 Genomes Project, leaving 29 variants. Genes that have been previously associated with SCID were checked manually because these could have been filtered out in the previous steps. These genes were also checked for the presence of compound heterozygous mutations, which were not detected. None of these known SCID genes was affected in any of the methods used. Using the trio analysis of patient and both parents, we selected SNVs that were not present in one of the parents as they were both asymptomatic for *de novo* autosomal dominant (AD) modeling. For autosomal recessive (AR) modeling, we filtered SNVs that were homozygous in the patient and heterozygous in at least one parent. X-linked modeling was comparable to AR modeling except that the mother was heterozygous for the SNV and that the SNV was not present in the father. These filtering steps resulted in 13 SNVs (Fig. 5A). Autosomal dominant (AD) *de novo* modeling resulted in a total 3 SNVs, autosomal recessive (AR) in 9 SNVs and X-linked recessive inheritance pattern in 1 SNV. PolyPhen²⁵ and SIFT²⁶ databases were used to determine whether variations were predicted as benign and tolerated in which case we did not consider them as being causative of the phenotype observed in the patient. Hereafter, we were left with 1 *de novo* SNV with a possible AD inheritance pattern. This SNV is located in *VPS4B* (vacuolar protein sorting 4 homolog B, NM_004869.3, NP_004860.2) encoding a heterozygous G to A mutation (c.869G>A) resulting in a predicted amino acid change at position 290 from arginine to glutamine (p.Arg290Gln). The variant is located in the AAA-ATPase domain of the protein²⁷, which is needed for proper function of *VPS4B*. Validation by Sanger sequencing verified the heterozygous genotype of the patient for the mutation in *VPS4B* and the absence of the SNV in both parents (Fig. 5B).

A

Exome Sequencing Data Filtering	
Aligned SNVs	381712
Nonsynonymous SNVs identified by 2 callers	88
SNVs not present in dbSNP or 100Genomes	29
SNVs not present in parents (AD modeling or heterozygous (AR modeling))	13
Damaging SNVs (PolyPhen & SIFT)	1

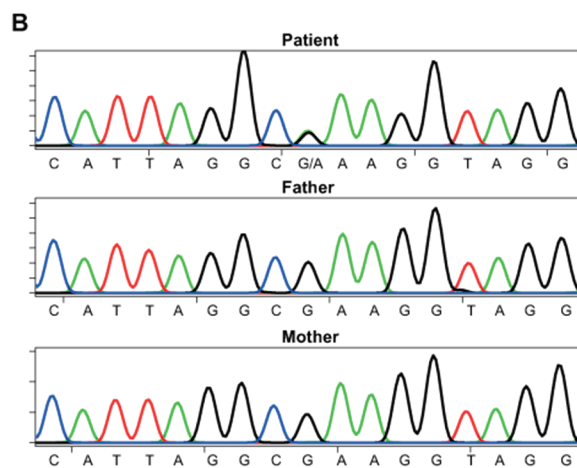


Figure 5: Detection of a *de novo* mutation in *VPS4B*. A) Filtering of data derived from exome sequencing of DNA from the patient and both parents. B) Sanger sequencing results of *VPS4B* gene in patient and both parents. Top; patient, middle; father, bottom; mother. AD; autosomal dominant, AR; autosomal recessive.

Discussion

Up to now, more than 16 genes have been identified to be causative for SCID that give rise to different phenotypes based on absence and presence of B cells and NK cells besides the T-cell deficiency². However, there remains a large fraction of patients with an unidentified underlying genetic defect and in addition still new SCID causing genes are being identified. Here, we describe a young patient with atypical presentation of SCID for who no mutation could be detected in genes known to be causative for SCID using standard Sanger sequencing protocols.

Previously, we have optimized the NSG humanized mouse model for efficient and robust engraftment of human BM derived HSPCs while maintaining multilineage differentiation and lymphocyte functionality¹⁸. In addition, we have used this model to determine the arrests in T-cell development for different types of SCID that were caused by a known underlying genetic defect. We also showed that the model faithfully recapitulates the arrests in B-cell development thereby validating this model for studies of human lymphoid development¹⁹. Here, we demonstrate the use of the NSG humanized mouse model for detection of SCID and determination of the stage of arrest in T-cell development. In addition, we confirmed that the patient with a suspected diagnosis of SCID indeed suffered from this disease with a T^BNK⁺ phenotype. When the patient was admitted to the intensive care unit, there was a drop in number of B cells that recovered to normal levels. In line with this, no aberrancies in B-cell development were observed in NSG mice transplanted with patient-derived HSPCs. We demonstrated that solely the T-cell lineage was affected and the arrest in T-cell development was found at the DP to SP transition with an accumulation of CD3⁺ DP at the expense of CD3⁺ DP. Arrests in T-cell development can also be studied using cocultures of HSPCs on OP9-DL1 stromal cells as this model is used to study normal T-cell development *in vitro*^{28, 29}. However, it remains difficult to reach the more mature stages, i.e. true DP stages and beyond, using these cultures. Therefore it would have been impossible to identify the late stage of arrest in human T-cell development that was identified here using the humanized mouse model.

A heterozygous microdeletion on chromosome 14 was found using a diagnostic SNP array CGH approach, however, this feature was also present in the father and therefore presumed unlikely to be pathogenic (data not shown). Therefore, we used whole exome sequencing to determine the causative defect using a trio analysis to exclude inherited polymorphisms, which were presumed unlikely to be causative. This approach has been proven successful in studies where they, for instance, identified a mutation in *CARD11* to be causative for SCID^{17, 30, 31}. Here, we filtered the data obtained with whole exome sequencing by using 2 different SNV callers, exclusion of SNVs present in either dbSNP or the 1000 Genomes Project and prediction of the possible effect of the SNV by PolyPhen and SIFT prediction tools. Furthermore, we excluded SNVs that were present in the parents. This step is crucial to come to disease-causing SNVs, because the genetic heterogeneity as well as low incidence of SCID make it impossible to analyze large numbers of phenotypically identical patient samples. Furthermore, it allowed us to screen for the presence of compound heterozygous mutations in genes known

to be associated with SCID, which were not found. In addition, by reporting single patient studies, other patients suffering from SCID without a known genetic cause can be screened for identified mutations as was also done for Bartter syndrome¹⁵. The use of whole exome sequencing technology for the use of diagnosis in orphan diseases such as SCID remains challenging and time consuming due to single patient analyses caused by low prevalence, however, we demonstrate here that it is possible.

After filtering of the exome data, we have identified a *de novo* heterozygous missense mutation in *VPS4B* in the patient that most likely has caused the observed immunodeficiency. The heterozygous mutation leads to a change in amino acids from Arginine to Glutamine at codon 290 and was confirmed by Sanger sequencing. We hypothesize that this might translate into a dominant negative form of VPS4B (dnVPS4B) as multiple dnVPS4B sequence variants have indeed been described that interfered with the normal function of VPS4B protein^{32, 33}. One described form of dnVPS4B has an amino acid change from the negatively charged glutamic acid to glutamine, which is uncharged and this mutation prevents binding of ATP³⁰. The mutation described here leads to a change of the positively charged amino acid arginine to the uncharged glutamine. It is possible that this change leads to a disruption of the function of the AAA-ATPase domain similar to the described dnVPS4B mutant, which had a mutation in the same domain and acts as dominant negative molecule preventing VPS4 function. VPS4B binds to the Endosomal Sorting Complexes Required for Transport (ESCRT)-III complex that is involved in multivesicular endosome (MVE) biogenesis and the final steps of vesicle fission³⁴. It has been described that VPS4B mediates scission of microvesicles that contain TCRs from the T-cell plasma membrane at the immunological synapse³². Furthermore, expression of a dnVPS4 disrupted the function of endogenous VPS4 resulting in an altered distribution of TCRs at the immunological synapse. In addition, we mined microarray data from sorted human thymus subsets³⁵ and it was observed that the expression of *VPS4B* increased in the SP stage of human T-cell development (Fig. 6). It is likely that the mutated *VPS4B* identified in the current study functions as a dominant negative mutant that interferes with endogenous VPS4B function, which is normally needed to progress to the SP stage of T-cell development. Moreover, thymocytes from mice that are double knockouts for *Stam1* and *Stam2*, components of the ESCRT-o complex that initiates the endosomal sorting process³⁴, have a block in T-cell development at the SP stage and these mice demonstrated defective proliferative responses after TCR stimulation³⁶. This demonstrates that processes in which ESCRT-complexes are involved, are needed for the transition from the CD3⁺ DP to the CD3⁺ DP and subsequent SP stage and most likely affect TCR signaling as also indicated by the observed decrease in CD5 expression.

The patient also suffered from neurological problems besides SCID, which are not possible to test in the humanized mouse model that was used in this study. However, it has been described that mutations in components of the ESCRT-III complex are involved in neurodegenerative diseases, such as amyotrophic lateral sclerosis and frontotemporal dementia (reviewed in³⁴). The involvement of the predicted p.Arg290Gln mutation in *VPS4B* in neuronal aberrancies could possibly be tested by generation of patient specific induced pluripotent stem cells

(iPSC) differentiated to the neuronal cell lineage³⁷. The same approach could be used together with the CRISPR/Cas9 technology³⁸ for site-directed repair of the mutation to determine whether this alleviates the phenotype. Unfortunately, it is still a challenge to differentiate repaired iPS cells into HSPCs that can be used for transplantation purposes in e.g. humanized mouse models.

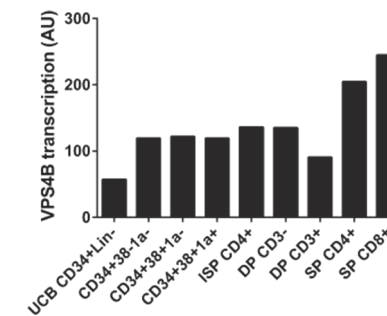


Figure 6: Expression of VPS4B in different stages of human T-cell development. Data was mined from microarray data of sorted populations from human thymus material³⁵.

To conclude, here we have identified a gene that potentially could be causative for T^B⁺NK⁻ SCID. A *de novo* G to A mutation at position c.869 resulting in an amino acid substitution from the negatively charged arginine to the uncharged glutamine that could result in a dnVPS4B protein was identified by exome sequencing of the index patient and both parents. Functional experiments are needed to confirm whether the identified dominant negative mutant indeed leads to an arrest in T-cell development. Furthermore, the NSG humanized mouse model was demonstrated to be useful in the determination whether the patient indeed suffered from SCID. Due to the long duration of the transplantation experiment, this will not be useful to aid in diagnosis. However, by identification of *VPS4B* as a potential candidate gene for SCID and after confirmation by functional experiments, this could be included for screening of other patients suffering from SCID without a known genetic cause³⁹.

References

1. Al-Herz W, Bousfiha A, Casanova JL, Chapel H, Conley ME, Cunningham-Rundles C, et al. Primary immunodeficiency diseases: an update on the classification from the international union of immunological societies expert committee for primary immunodeficiency. *Frontiers in immunology* 2011, **2**: 54.
2. Bousfiha A, Jeddane L, Al-Herz W, Ailal F, Casanova JL, Chatila T, et al. The 2015 IUIS Phenotypic Classification for Primary Immunodeficiencies. *Journal of clinical immunology* 2015.
3. Buckley RH, Schiff RI, Schiff SE, Markert ML, Williams LW, Harville TO, et al. Human severe combined immunodeficiency: genetic, phenotypic, and functional diversity in one hundred eight infants. *The Journal of pediatrics* 1997, **130**(3): 378-387.
4. Yee A, De Ravin SS, Elliott E, Ziegler JB, Contributors to the Australian Paediatric Surveillance U. Severe combined immunodeficiency: a national surveillance study. *Pediatric allergy and immunology : official publication of the European Society of Pediatric Allergy and Immunology* 2008, **19**(4): 298-302.
5. Aiuti A, Cattaneo F, Galimberti S, Benninghoff U, Cassani B, Callegaro L, et al. Gene therapy for immunodeficiency due to adenosine deaminase deficiency. *The New England journal of medicine* 2009, **360**(5): 447-458.
6. Gaspar HB, Cooray S, Gilmour KC, Parsley KL, Zhang F, Adams S, et al. Hematopoietic stem cell gene therapy for adenosine deaminase-deficient severe combined immunodeficiency leads to long-term immunological recovery and metabolic correction. *Science translational medicine* 2011, **3**(97): 97ra80.
7. Gaspar HB, Parsley KL, Howe S, King D, Gilmour KC, Sinclair J, et al. Gene therapy of X-linked severe combined immunodeficiency by use of a pseudotyped gammaretroviral vector. *Lancet* 2004, **364**(9452): 2181-2187.
8. Hacein-Bey-Abina S, Le Deist F, Carlier F, Bouneaud C, Hue C, De Villartay JP, et al. Sustained correction of X-linked severe combined immunodeficiency by ex vivo gene therapy. *The New England journal of medicine* 2002, **346**(16): 1185-1193.
9. Hacein-Bey-Abina S, Pai SY, Gaspar HB, Arman M, Berry CC, Blanche S, et al. A modified gamma-retrovirus vector for X-linked severe combined immunodeficiency. *The New England journal of medicine* 2014, **371**(15): 1407-1417.
10. Gaspar HB, Qasim W, Davies EG, Rao K, Amrolia PJ, Veys P. How I treat severe combined immunodeficiency. *Blood* 2013, **122**(23): 3749-3758.
11. Alsmadi O, Al-Ghoniaim A, Al-Muhsen S, Arnaout R, Al-Dhekri H, Al-Saud B, et al. Molecular analysis of T-B-NK+ severe combined immunodeficiency and Omenn syndrome cases in Saudi Arabia. *BMC medical genetics* 2009, **10**: 116.
12. Kwan A, Church JA, Cowan MJ, Agarwal R, Kapoor N, Kohn DB, et al. Newborn screening for severe combined immunodeficiency and T-cell lymphopenia in California: results of the first 2 years. *The Journal of allergy and clinical immunology* 2013, **132**(1): 140-150.
13. Pasic S, Vujic D, Veljkovic D, Slavkovic B, Mostarica-Stojkovic M, Minic P, et al. Severe combined immunodeficiency in Serbia and Montenegro between years 1986 and 2010: a single-center experience. *Journal of clinical immunology* 2014, **34**(3): 304-308.
14. Yu GP, Nadeau KC, Berk DR, de Saint Basile G, Lambert N, Knapnougel P, et al. Genotype, phenotype, and outcomes of nine patients with T-B+NK+ SCID. *Pediatric transplantation* 2011, **15**(7): 733-741.
15. Choi M, Scholl UI, Ji W, Liu T, Tikhonova IR, Zumbo P, et al. Genetic diagnosis by whole exome capture and massively parallel DNA sequencing. *Proceedings of the National Academy of Sciences of the United States of America* 2009, **106**(45): 19096-19101.
16. Ng SB, Buckingham KJ, Lee C, Bigham AW, Tabor HK, Dent KM, et al. Exome sequencing identifies the cause of a mendelian disorder. *Nature genetics* 2010, **42**(1): 30-35.
17. Greil J, Rausch T, Giese T, Bandapalli OR, Daniel V, Bekeredjian-Ding I, et al. Whole-exome sequencing links caspase recruitment domain 11 (CARD11) inactivation to severe combined immunodeficiency. *The Journal of allergy and clinical immunology* 2013, **131**(5): 1376-1383 e1373.
18. Wiekmeijer AS, Pike-Overzet K, Brugman MH, Salvatori DC, Egeler RM, Bredius RG, et al. Sustained Engraftment of Cryopreserved Human Bone Marrow CD34(+) Cells in Young Adult NSG Mice. *BioResearch open access* 2014, **3**(3): 110-116.
19. Wiekmeijer AS, Pike-Overzet K, H IJ, Brugman MH, Wolvers-Tettero IL, Lankester AC, et al. Identification of checkpoints in human T-cell development using severe combined immunodeficiency stem cells. *The Journal of allergy and clinical immunology* 2015.
20. Noordzij JG, de Bruin-Versteeg S, Verkaik NS, Vossen JM, de Groot R, Bernatowska E, et al. The immunophenotypic and immunogenotypic B-cell differentiation arrest in bone marrow of RAG-deficient SCID patients corresponds to residual recombination activities of mutated RAG proteins. *Blood* 2002, **100**(6): 2145-2152.
21. DePristo MA, Banks E, Poplin R, Garimella KV, Maguire JR, Hartl C, et al. A framework for variation discovery and genotyping using next-generation DNA sequencing data. *Nature genetics* 2011, **43**(5): 491-498.
22. Li H, Durbin R. Fast and accurate short read alignment with Burrows-Wheeler transform. *Bioinformatics* 2009, **25**(14): 1754-1760.
23. Li H, Handsaker B, Wysoker A, Fennell T, Ruan J, Homer N, et al. The Sequence Alignment/Map format and SAMtools. *Bioinformatics* 2009, **25**(16): 2078-2079.
24. Azzam HS, Grinberg A, Lui K, Shen H, Shores EW, Love PE. CD5 expression is developmentally regulated by T cell receptor (TCR) signals and TCR avidity. *The Journal of experimental medicine* 1998, **188**(12): 2301-2311.
25. Adzhubei IA, Schmidt S, Peshkin L, Ramensky VE, Gerasimova A, Bork P, et al. A method and server for predicting damaging missense mutations. *Nature methods* 2010, **7**(4): 248-249.
26. Kumar P, Henikoff S, Ng PC. Predicting the effects of coding non-synonymous variants on protein function using the SIFT algorithm. *Nature protocols* 2009, **4**(7): 1073-1081.
27. Takasu H, Jee JG, Ohno A, Goda N, Fujiwara K, Tochio H, et al. Structural characterization of the MIT domain from human Vps4b. *Biochemical and biophysical research communications* 2005, **334**(2): 460-465.
28. De Smedt M, Leclercq G, Vandekerckhove B, Kerre T, Tagnon T, Plum J. T-lymphoid differentiation potential measured in vitro is higher in CD34+CD38-/lo hematopoietic stem cells from umbilical cord blood than from bone marrow and is an intrinsic property of the cells. *Haematologica* 2011, **96**(5): 646-654.
29. La Motte-Mohs RN, Herer E, Zuniga-Pflucker JC. Induction of T-cell development from human cord blood hematopoietic stem cells by Delta-like 1 in vitro. *Blood* 2005, **105**(4): 1431-1439.

30. Bernth-Jensen JM, Holm M, Christiansen M. Neonatal-onset TBNK severe combined immunodeficiency and neutropenia caused by mutated phosphoglucomutase 3. *The Journal of allergy and clinical immunology* 2015.
31. Frugoni F, Dobbs K, Felgentreff K, Aldhekri H, Al Saud BK, Arnaout R, et al. A novel mutation in the POLE2 gene causing combined immunodeficiency. *The Journal of allergy and clinical immunology* 2015.
32. Choudhuri K, Llodra J, Roth EW, Tsai J, Gordo S, Wucherpfennig KW, et al. Polarized release of T-cell-receptor-enriched microvesicles at the immunological synapse. *Nature* 2014, **507**(7490): 118-123.
33. Garrus JE, von Schwedler UK, Pornillos OW, Morham SG, Zavitz KH, Wang HE, et al. Tsg101 and the vacuolar protein sorting pathway are essential for HIV-1 budding. *Cell* 2001, **107**(1): 55-65.
34. Rusten TE, Vaccari T, Stenmark H. Shaping development with ESCRTs. *Nature cell biology* 2012, **14**(1): 38-45.
35. Dik WA, Pike-Overzet K, Weerkamp F, de Ridder D, de Haas EF, Baert MR, et al. New insights on human T cell development by quantitative T cell receptor gene rearrangement studies and gene expression profiling. *The Journal of experimental medicine* 2005, **201**(11): 1715-1723.
36. Yamada M, Ishii N, Asao H, Murata K, Kanazawa C, Sasaki H, et al. Signal-transducing adaptor molecules STAM1 and STAM2 are required for T-cell development and survival. *Molecular and cellular biology* 2002, **22**(24): 8648-8658.
37. Chamberlain SJ, Li XJ, Lalande M. Induced pluripotent stem (iPS) cells as in vitro models of human neurogenetic disorders. *Neurogenetics* 2008, **9**(4): 227-235.
38. Jinek M, Chylinski K, Fonfara I, Hauer M, Doudna JA, Charpentier E. A programmable dual-RNA-guided DNA endonuclease in adaptive bacterial immunity. *Science* 2012, **337**(6096): 816-821.
39. Casanova JL, Conley ME, Seligman SJ, Abel L, Notarangelo LD. Guidelines for genetic studies in single patients: lessons from primary immunodeficiencies. *The Journal of experimental medicine* 2014, **211**(11): 2137-2149.